Acta Cryst. (1977). B33, 2767–2775

Crystal Structure and Ionic Conductivity of Li Boracites

BY W. JEITSCHKO,* T. A. BITHER AND P. E. BIERSTEDT

Central Research and Development Department,† E. I. du Pont de Nemours and Company, Wilmington, Delaware 19898, *USA*

(*Received* 27 *January* 1977; *accepted* 26 *February* 1977)

$Li_4B_7O_{12}Cl$ crystallizes in three modifications which transform into each other by displacive phase transitions. The γ form, stable above 348 K, is cubic, $F\bar{4}3c$, $a = 12{\cdot}167$ (3) Å, $Z = 8$. Its structure was determined from high-temperature (353 K) single-crystal counter data and refined with anisotropic thermal parameters to an R of 0·027 for 190 structure factors. The structure differs from that of the mineral boracite, $Mg_3B_7O_{13}Cl$, mainly in the position of the additional Li and the absence of a set of O atoms. The Li^+ ions show characteristics of high mobility: they are located in channels which are suited as diffusion paths, their sites have fractional occupancy, and they have large thermal amplitudes. Li^+ conductivity was demonstrated in a DC electrochemical cell consisting of two compartments of Li amalgam separated by a polycrystalline platelet of $Li_4B_7O_{12}Cl_{0{\cdot}68}Br_{0{\cdot}32}$. This Li boracite is in the γ form at room temperature, where its ionic conductivity is about $2 \times 10^{-6}\ \Omega^{-1}\ cm^{-1}$. The temperature dependence of the conductivity was monitored by AC conductance and capacitance measurements. Above 600 K the ionic conductivities of the Li boracites approach those of the best known solid electrolytes. β-$Li_4B_7O_{12}Cl$, stable between 310 and 348 K, crystallizes in space group $P\bar{4}3n$ with $a = 12{\cdot}161$ (3) Å. The α form, stable below 310 K, has a rhombohedrally distorted lattice, space group $R3$, with $a = 12{\cdot}1410$ (8) Å, $\alpha = 90{\cdot}083$ (8)°. The face-centered cubic substructures of the β and α forms of $Li_4B_7O_{12}Cl$ were refined from single-crystal counter data.

Introduction

The compounds known as boracites generally have the formula $M_3B_7O_{13}X$, where M = Mg, Cr, Mn, Fe, Co, Ni, Zn or Cd, and X = Cl, Br or I. Most boracites undergo displacive phase transitions from a high-temperature cubic structure to structures of orthorhombic, trigonal, or monoclinic symmetry and, therefore, have interesting physical properties (Nelmes, 1974).

Recently Li-containing compounds were prepared which have the somewhat different composition $Li_4B_7O_{12}X$, where X = Cl, Br (Levasseur, Fouassier & Hagenmuller, 1971), or I (Jeitschko & Bither, 1972). Their structure contains the same B_7O_{12} framework as found by Ito, Morimoto & Sadanaga (1951) for boracite, $Mg_3B_7O_{13}Cl$. We have refined the structure of $Li_4B_7O_{12}Cl$ from data collected at three different temperatures corresponding to its three modifications (Jeitschko & Bither, 1972). The results suggested high mobility for the Li atoms which we have subsequently proven and studied in an electrochemical cell (Bither & Jeitschko, 1975). The present paper gives a detailed account of our work.

* Present address: Institut für Anorganische und Analytische Chemie, Justus-Liebig-Universität, 6300 Giessen, Federal Republic of Germany.

† Contribution No. 2437.

Sample preparation and crystal growth

$Li_4B_7O_{12}Cl$ and $Li_4B_7O_{12}Br$ were obtained in the form of microcrystalline powders by heating B_2O_3/Li_2O mixtures in molar ratios from about 7/4 to 7/2 at about 900 K in an excess of fused LiCl or LiBr. The method does not appear to work with LiI. The haloboracite compounds can be separated by washing with water, in which the Li haloboracites are relatively insoluble. The purities of the chemicals used were of reagent grade or better.

To obtain the Li haloboracites as clear crystals of macroscopic size hydrothermal methods were used. For the chloro- and bromoboracites a pressure of about 3 kbar suffices, while for iodoboracites higher pressures of about 30 kbar were used. After contact of the reactants for several hours at about 950 K under pressure the mixture was slowly cooled (*e.g.* 10–30 K h^{-1}).

Reactions at 3 kbar are conveniently carried out by sealing the appropriate reactants in Au tubes. These tubes are then placed in a bomb, pressurized with argon, and heated. The argon pressure and bomb temperature are adjusted to give the desired reaction conditions. Reactions at a higher pressure were carried out in a piston–cylinder device (Boyd & England, 1960) where the reactants are sealed in a container made of Pt or Au tubing. Good hydrothermal growth

conditions were observed with a H_2O/B ratio of about 0·2 to 0·5. Water was added as a hydrate of one of the reactants. An infrared spectrum of $Li_4B_7O_{12}Cl$ showed no bands characteristic of OH or H_2O.

In Li boracites with mixed halogens the proportion of the various halogens in the product is determined principally by their respective proportions in the starting mixture. In the solid solution $Li_4B_7O_{12}Cl_{1-x}Br_x$ we observed a tendency for a larger proportion of the smaller halogen, Cl, to be incorporated in the product, as found by chemical analysis. Within the error limits of the chemical analysis the (pseudocubic) lattice constants followed Vegard's rule.

Optical and thermal investigations

Crystals of $Li_4B_7O_{12}Cl$ were examined on a hot-stage microscope with polarized light. They are colorless, clear, and double-diffracting at room temperature and become optically isotropic on heating, with a transition at about 310 K. The onset of the transition is noticeable about 3 K earlier, although the final step occurs abruptly, indicating a first-order transition. The transition temperatures vary from one batch to another by ±5 K, but less so from crystal to crystal within one batch. The crystals remain optically isotropic on further heating, which was continued to 400 K. On cooling to room temperature they become anisotropic only after several hours.

Differential scanning calorimetry of $Li_4B_7O_{12}Cl$ shows two endotherms: the transition at about 310 K and another at about 348 K. While this latter transition is rapidly reversible with no obvious hysteresis, the lower transition could not be observed on cooling, thus confirming its sluggishness. The heat of transformation observed on heating is about the same for both transitions. The onset of decomposition of $Li_4B_7O_{12}Cl$ was observed at a temperature around 1140 K. We will call the modification of $Li_4B_7O_{12}Cl$ which is stable at room temperature the α form; the modifications stable from 310 to 348 K and above 348 K will be designated β and γ respectively.

Crystals of $Li_4B_7O_{12}Br$ and $Li_4B_7O_{12}I$ are also optically anisotropic at room temperature. By differential scanning calorimetry, both show single, rapidly reversible transitions with sharp endotherms peaking at around 500 and 540 K respectively.

Crystals of the solid solution $Li_4B_7O_{12}Cl$–$Li_4B_7O_{12}Br$ resemble those of $Li_4B_7O_{12}Br$ in that they usually show one transition by differential scanning calorimetry, whereas two are observed for $Li_4B_7O_{12}Cl$. The transition temperature goes through a minimum below room temperature for crystals with a molar Cl/Br ratio of around 70/30.

Lattice constants

Debye–Scherrer films and routine powder-diffractometer scans of the Li haloboracites show patterns typical of the cubic boracite structure. Even strongly exposed Guinier patterns obtained with a Hägg-type camera and Cu $K\alpha_1$ radiation do not show superstructure reflections for any of the three Li haloboracites, although they were observed later on single-crystal patterns of $Li_4B_7O_{12}Cl$. The pseudocubic lattice constants of the three Li haloboracites refined from the Guinier–Hägg data with high-purity KCl (a = 6·2931 Å) as standard are a = 12·144, 12·190 and 12·273 Å for the Cl, Br and I compounds respectively. Standard deviations of these refinements are less than 0·001 Å, although variations of ±0·005 Å were observed in different preparations.

Since the optically observed anisotropy is incompatible with cubic symmetry, the Guinier films were carefully examined for evidence of lower symmetry. The films of the Li–Br boracite show resolved line splitting and the splitting characteristics clearly indicate rhombohedral symmetry. Thus, for instance, the cubic $h00$ reflections do not split (Table 1). Guinier films of the Li–Cl boracite show slight diffuseness and broadening for freshly ground samples. We suspected that grinding transformed the samples, at least partially,* to the optically isotropic β modification, which is stable

* This phase transition might be induced not only by locally reaching the transition temperature (which is only slightly above room temperature) but also by mechanical stress, since the phase stable at room temperature is ferroelastic, and switching will go through the higher-symmetry, high-temperature structure.

Table 1. *Evaluation of a Guinier–Hägg powder pattern of* $Li_4B_7O_{12}Br$ *recorded with* Cu $K\alpha_1$ *radiation*

Intensities were calculated with the positional parameters of γ-$Li_4B_7O_{12}Cl$ as found in the single-crystal study. The first column contains the indices for this cubic subcell.

cubic F hkl	trigonal R h k l	rhombohedral h k l	d_c	d_o	I_c	I_o
200	2 0 2	2 0 0	6.0933	6.0891	5	w
220	2 2 0	2 0-2	4.3113	4.3057	5	m
	0 2 4	2 2 0	4.3059		5	
222	0 4 2	2 2-2	3.5194	3.5198	75	vvs
	0 0 6	2 2 2	3.5145	3.5144	25	vs
400	4 0 4	4 0 0	3.0466	3.0469	16	s
420	4 2 2	4 0-2	2.7264	2.7248	43	vvs
	2 2 6	4 2 0	2.7236		43	
422	1 0 0	4-2-2	2.4891	2.4881	12	vs
	2 4 4	4 2-2	2.4881		24	
	2 0 8	4 2 2	2.4850	2.4857	12	s
440	4 4 0	4 0-4	2.1557	2.1550	7	w
	0 4 8	4 4 0	2.1529	2.1521	7	w
531	6 2 1	5-1-3	2.0612	2.0607	13	vs
	4 4 3	5 1-3	2.0609		13	
	2 4 7	5 3-1	2.0594	2.0592	13	vs
	2 2 9	5 3 1	2.0582		13	
600	2 6 2	4 2-4	2.0322	2.0315	4	w,d
442	6 0 6	6 0 0	2.0311		2	
	0 4 8	4 4 0	2.0311		2	
620	0 210	4 4 2	2.0288		2	-
	6 2 4	6 0-2	1.9276	1.9276	9	m
	4 2 8	6 2 0	1.9261	1.9263	9	m
	8 0 2	6-2-2	1.8382		2	
622	4 4 6	6 2-2	1.8374	1.8376	4	w
	4 010	6 2 2	1.8357		2	
444	0 8 4	4 4-4	1.7597	1.7600	9	m
	0 012	4 4 4	1.7588	1.7567	3	vw
640	6 4 2	6 0-4	1.6910	1.6912	9	m
	2 410	6 4 0	1.6890	1.6889	9	m
	8 2 0	6-2-4	1.6295		2	
642	4 6 4	6 2-4	1.6292	1.6292	5	s
	2 6 8	6 4-2	1.6283		2	
	2 212	6 4 2	1.6269	1.6272	5	s
	2 3 7	7-1-3	1.5874		1	
731	6 4 5	7 1-3	1.5871	1.5872	1	vw,d
	4 4 9	7 3-1	1.5862		1	
	4 211	7 3 1	1.5855		1	
800	8 0 8	8 0 0	1.5233	1.5237	4	vw
	010 2	4 4-6	1.4787		3	
644	2 8 6	6 4-4	1.4783	1.4782	6	vs
820	8 2 6	8 0-2	1.4783		8	
	6 210	8 2 0	1.4774		8	
	2 014	6 4 4	1.4761	1.4763	3	w
	6 6 0	6 0-6	1.4371		1	
660	10 0 4	8-2-2	1.4369		1	
822	6 4 8	8 2-2	1.4363	1.4366	1	vw
	0 612	6 6 0	1.4353		1	
	6 012	8 2 2	1.4353		1	
	8 4 1	7-1-5	1.4081		1	-
751	6 6 3	7 1-5	1.4080		1	-
	2 611	7 5-1	1.4066		1	-
	2 413	7 5 1	1.4061		1	-
	4 8 2	6 2-6	1.3987	1.3985	4	w
662	0 810	6 6-2	1.3976	1.3970	2	vw
	0 414	6 6 2	1.3965		2	
840	8 4 4	8 0-4	1.3632	1.3629	4	w
	4 412	8 4 0	1.3618	1.3616	4	w
	210 1	5 3-7	1.3385	1.3383	1	vvw
753	4 8 5	7 3-5	1.3382		1	
	2 8 9	7 5-3	1.3377	1.3357	1	vvw
	2 215	7 5 3	1.3362		1	
	10 2 2	8-2-4	1.3305	1.3302	2	w
842	6 6 6	8 2-4	1.3301		2	
	4 610	8 4-2	1.3295	1.3288	2	w
	4 214	8 4 2	1.3286		2	

above 310 K. Since the inverse transformation is very sluggish, such samples would not have reached equilibrium at the time the X-ray patterns were recorded. Although this point was not studied in detail, a Guinier pattern recorded from a sample mounted several days in advance showed line splitting with the same rhombohedral characteristics observed for the Li–Br boracite. Least-squares refinement of the resolved lines resulted in the rhombohedral lattice constants a = 12·1410 (8) Å, α = 90·083 (8)°, and a = 12·1866 (6) Å, α = 90·072 (6)° for the Cl and Br compounds respectively. Corresponding trigonal lattice constants are a = 17·182, c = 20·998 Å and a = 17·245, c = 21·081 Å.

To obtain lattice constants for the high-temperature modifications of $Li_4B_7O_{12}Cl$, precession photographs recorded at room temperature, 328, and 353 K under otherwise identical conditions were evaluated. From the relative positions of corresponding reflections and the known (from Guinier data) lattice constants at room temperature, the lattice constants of the high-temperature modifications were calculated. Averages of several measurements were a = 12·161 (3) Å at 328 K and a = 12·167 (3) Å at 353 K.

Crystal structure of γ-$Li_4B_7O_{12}Cl$ at 353 K (prototypic structure)

Experimental

The single crystals of $Li_4B_7O_{12}Cl$ used for the structural studies were grown hydrothermally. They were mounted with an epoxy adhesive on thin glass fibers and heated to the desired temperature by a hot-air gun (Jeitschko, 1972). Buerger precession diagrams taken with Mo $K\alpha$ radiation above 350 K show the reflection characteristics of space groups $F\bar{4}3c$ and $Fm3c$: hkl only with $h+k$, $k+l$, $l+h = 2n$; hhl only with $l = 2n$. $F\bar{4}3c$ is the prototypic space group for all boracites with 'normal' composition. It was found to be correct also for $Li_4B_7O_{12}Cl$ in its high-temperature form.

The crystal selected for the intensity measurements was of irregular shape with overall dimensions between 0·15 and 0·25 mm. A four-circle diffractometer was used with graphite-monochromatized Mo $K\alpha$ radiation, a scintillation counter, and a pulse-height discriminator. Scans were along 2θ extending over 2·2° plus the angular separation of the $K\alpha$ doublet, with a scan speed of $1°2\theta$ min^{-1} and background counts of 20 s at both sides of each scan. The intensity of a standard reflection varied ±3% over the period of data collection. All reflections of one octant up to $2\theta = 70°$ were measured. Because of the low absorption coefficient (μ = 5·5 cm^{-1}) no absorption correction was made. The largest errors in structure factors due to this neglect were calculated to be less than ±1·5%. Averaging over the (generally) six equivalent reflections within one octant reduced these errors.

Structure determination and refinement

It was clear that the structure of $Li_4B_7O_{12}Cl$ is closely related to that of the mineral boracite, $Mg_3B_7O_{13}Cl$ (Ito, Morimoto & Sadanaga, 1951). The structure was therefore determined by subsequent least-squares refinements and difference syntheses.

Table 2. *Positional and thermal parameters of* $Li_4B_7O_{12}Cl$ *at different temperatures*

The data given for 298 and 328 K correspond to the $F\bar{4}3c$ subcell, which is the true cell above 348 K. Vibrational parameters (×10^5) are defined by $T = \exp(-\Sigma\Sigma\, h_i h_j b_{ij})$. Equivalent isotropic parameters, B(Å^2), are also listed. Numbers in parentheses are e.s.d.'s in the least significant digits. The last column contains R for the structure amplitudes (in parentheses) with non zero weight in the least-squares refinements, and the total number of F's respectively.

Temperature (K)		$F\bar{4}3c$	Occupation	x	y	z	b_{11}	b_{22}	b_{33}	b_{12}	b_{13}	b_{23}	B	R(Number of F's)
353	Li(1)	32(*e*)	0·316 (32)	0·86425 (85)	x	x	330 (71)	b_{11}	b_{11}	−67 (42)	b_{12}	b_{12}	1·94	0·025 (179)
(γ)	Li(2)	24(*c*)	0·937 (39)	0	¼	¼	2679 (181)	236 (33)	b_{22}	0	0	0	6·19	0·027 (190)
	B(1)	24(*d*)	1	¼	0	0	86 (9)	95 (6)	b_{22}	0	0	0	0·54	
	B(2)	32(*e*)	1	0·10083 (10)	x	x	106 (5)	b_{11}	b_{11}	10 (4)	b_{12}	b_{12}	0·62	
	O	96(*h*)	1	0·02263 (7)	0·09769 (6)	0·18207 (7)	124 (5)	121 (4)	124 (5)	35 (3)	57 (3)	44 (4)	0·73	
	Cl	8(*b*)	1	¼	¼	¼	273 (3)	b_{11}	b_{11}	0	0	0	1·61	
328	Li(1)	32(*e*)	0·278 (34)	0·86533 (94)	x	x	254 (84)	b_{11}	b_{11}	−60 (46)	b_{12}	b_{12}	1·45	0·025 (152)
(β)	Li(2)	24(*c*)	0·967 (43)	0	¼	¼	2781 (194)	232 (37)	b_{22}	0	0	0	6·37	0·028 (159)
	B(1)	24(*d*)	1	¼	0	0	79 (10)	92 (7)	b_{22}	0	0	0	0·52	
	B(2)	32(*e*)	1	0·10089 (12)	x	x	111 (6)	b_{11}	b_{11}	11 (6)	b_{12}	b_{12}	0·66	
	O	96(*h*)	1	0·02258 (8)	0·09788 (7)	0·18213 (8)	124 (6)	120 (5)	121 (6)	31 (4)	52 (4)	45 (5)	0·72	
	Cl	8(*b*)	1	¼	¼	¼	262 (4)	b_{11}	b_{11}	0	0	0	1·55	
298	Li(1)	32(*e*)	½	0·87079 (159)	x	x	559 (429)	b_{11}	b_{11}	−560 (250)	b_{12}	b_{12}	Negative	0·122 (187)
(α)	Li(2)	24(*c*)	1	0	¼	¼	5754 (1832)	2 (68)	b_{22}	0	0	0	11·3	0·122 (189)
	B(1)	24(*d*)	1	¼	0	0	194 (56)	167 (38)	b_{22}	0	0	0	1·04	
	B(2)	32(*e*)	1	0·10036 (48)	x	x	157 (27)	b_{11}	b_{11}	−17 (24)	b_{12}	b_{12}	0·93	
	O	96(*h*)	1	0·02252 (36)	0·09813 (37)	0·18172 (36)	162 (28)	192 (27)	176 (27)	−5 (20)	66 (18)	80 (21)	1·04	
	Cl	8(*b*)	1	¼	¼	¼	262 (18)	b_{11}	b_{11}	0	0	0	1·55	

A full-matrix least-squares program (Finger, 1969) was used which minimizes $\Sigma w(KF_o - |F_c|)^2$, where w is the weight based on counting statistics and K is a scale factor. Scattering factors for neutral atoms were taken from Cromer & Mann (1968), and corrected for anomalous dispersion (Cromer & Liberman, 1970). The difference syntheses were calculated with a program by Fritchie & Guggenberger (1967). Secondary extinction was corrected for by Zachariasen's (1963) model. Reflections for which this correction amounted to more than 25% and reflections which were measured as smaller than three standard deviations were assigned zero weight in the least-squares refinement. They are marked with an asterisk in the list of observed and calculated structure factors.*

Table 3. *Interatomic distances* (Å) *and angles* (°) *in* γ-$Li_4B_7O_{12}Cl$ *at* 353 K

Standard deviations, computed from e.s.d.'s of positional parameters and lattice constants, are all less than 0·015 Å and 1·0°. All distances less than 2·35 Å are listed. Shortest Li–Li, Li–B, B–B, and O–O distances are 2·57, 2·72, 2·51, and 2·38 Å respectively.

Li(1)–3 O	2·060	O–Li(1)–O	96·2 (3x)
–1 Cl	2·408	O–Li(1)–Cl	120·8 (3x)
Li(2)–4 O	2·048	O–Li(2)–O	91·0 (4x)
–2 Cl	3·042	O–Li(2)–O	164·5 (2x)
B(1)–4 O	1·474	O–B(1)–O	108·3 (4x)
B(2)–3 O	1·373	O–B(1)–O	111·8 (2x)
O–1 Li(1)	2·060	O–B(2)–O	120·0 (3x)
–1 Li(2)	2·048	Li(1)–O–Li(2)	77·4 (1x)
–1 B(1)	1·474	Li(1)–O–B(1)	99·2 (1x)
–1 B(2)	1·373	Li(1)–O–B(2)	116·4 (1x)
Cl–4 Li(1)	2·408	Li(2)–O–B(1)	118·6 (1x)
–6 Li(2)	3·042	Li(2)–O–B(2)	111·0 (1x)
		B(1)–O–B(2)	123·8 (1x)
		Li(1)–Cl–Li(1)	109·5 (6x)

According to the formula composition, 32 Li atoms need to be placed in the $F\bar{4}3c$ cell. They were found in positions 24(*c*) (which corresponds to the positions of the Mg atoms of $Mg_3B_4O_{13}Cl$) and 32(*e*). Least-squares refinement and difference syntheses showed large thermal parameters and partial occupancies for both these positions. In the final cycles, the occupancy and thermal parameters of these Li positions were varied simultaneously. The Li content calculated from the occupancy parameters (Table 2) is within 2% of the formula composition ($0{\cdot}316 \times 32/8 + 0{\cdot}937 \times 24/8 = 4{\cdot}075$ Li atoms per formula unit).

As a check for absolute configuration, several least-squares cycles were run with indices hkl changed to $\bar{h}\bar{k}\bar{l}$. The resulting R was 0·029, compared with 0·027 for the correct orientation. Both values correspond to the total of 190 structure factors. For the 179 structure factors with non-zero weight, $R = 0{\cdot}025$. The results of this refinement are given in Tables 2 and 3, and Figs. 1 and 2.

In a final difference synthesis the strongest peaks were one-tenth as high as those for a fully occupied Li position in a previous Fourier synthesis. These peaks

* A list of structure factors at 353, 328 and 298 K has been deposited with the British Library Lending Division as Supplementary Publication No. SUP 32562 (4 pp.). Copies may be obtained through The Executive Secretary, International Union of Crystallography, 13 White Friars, Chester CH1 1NZ, England.

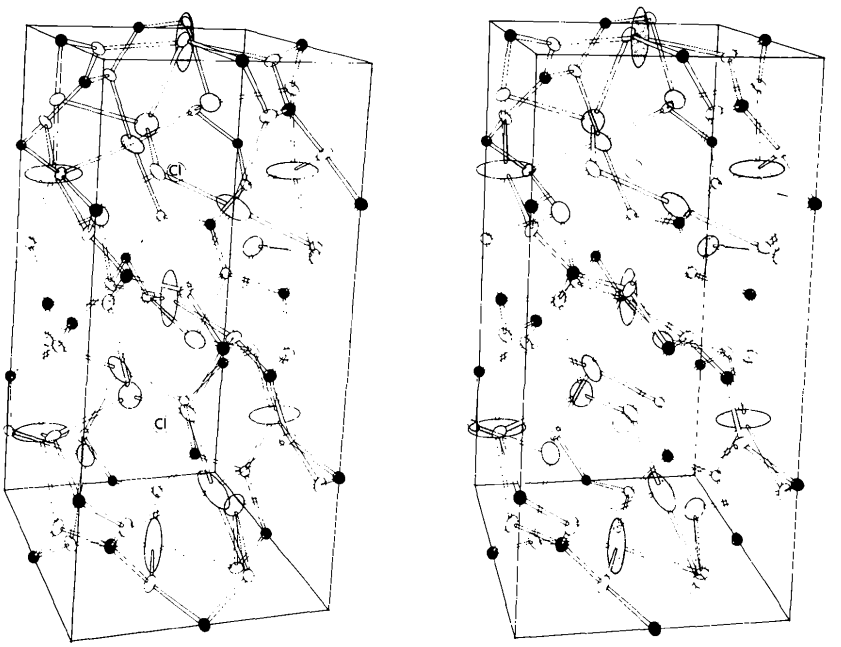

Fig. 1. Stereo-drawing of $Li_4B_7O_{12}Cl$ at 353 K. Two octants of the $F\bar{4}3c$ cell were drawn with *ORTEP* (Johnson, 1965). The thermal ellipsoids correspond to the 50% probability limit. Li atoms are shaded, B and O atoms are black and white respectively.

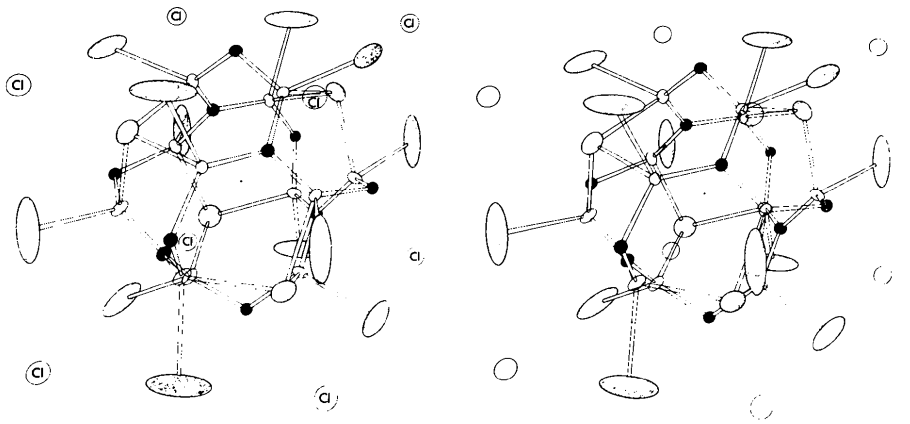

Fig. 2. Stereo-drawing of $Li_4B_7O_{12}Cl$ at 353 K. One-eighth of the face-centered cell is shown. The dot at the center of the drawing marks the O position of $Mg_3B_7O_{13}Cl$, which is unoccupied in $Li_4B_7O_{12}Cl$. This position corresponds to the corners of the octants of Fig. 1.

were located in the B(1)–O and B(2)–O bonds indicating their partial covalency. Similar residual electron densities were observed in other light-atom structure refinements of high accuracy (Göttlicher & Wölfel, 1959; O'Connell, Rae & Maslen, 1966; Coppens & Vos, 1971).

On the crystal structures of α- and β-$Li_4B_7O_{12}Cl$

Precession diagrams of α- and β-$Li_4B_7O_{12}Cl$ were recorded at 298 and 328 K respectively. In addition to the strong subcell reflections of the face-centered prototypic (γ) structure these diagrams showed weak superstructure reflections for both the α and β forms. With these additional reflections the cells became primitive. The deviations from cubic symmetry observed for α-$Li_4B_7O_{12}Cl$ in the Guinier films described above were too small to be noticeable on the precession diagrams. On the other hand, the intensities of the superstructure reflections recorded on the precession films were too low to be observable on the Guinier diagrams.

The space group of β-$Li_4B_7O_{12}Cl$

The crystal used for the collection of the 353 K data was first employed to measure single-crystal counter data at 328 K. All possible reflections of one octant of the primitive cubic cell were measured up to $2\theta = 65°$, with the experimental setup described above. Systematic extinctions occurred for reflections hkl, which were observed only for $l = 2n$. Thus the space group is uniquely determined as $P\bar{4}3n$, since it has to be a subgroup of the prototypic group $F\bar{4}3c$ (Fig. 3). This group is also consistent with the optical properties described above.

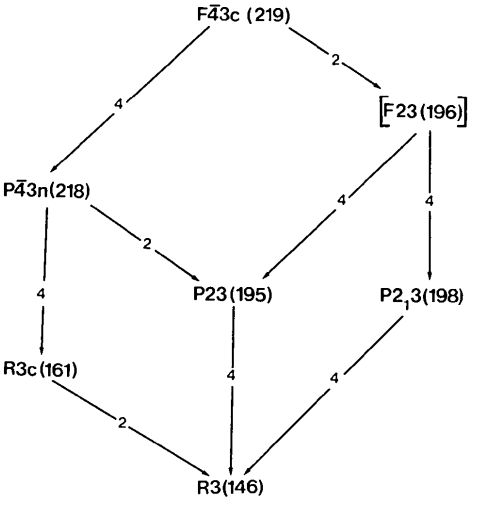

Fig. 3. Cubic and rhombohedral subgroups of $F\bar{4}3c$ with translational symmetry as observed on precession diagrams of α- and β-$Li_4B_7O_{12}Cl$. The groups (with their numbers in parentheses) are connected by arrows containing the index of the subgroup.

The space group of α-$Li_4B_7O_{12}Cl$

The space group of $Li_4B_7O_{12}Cl$ at room temperature must be rhombohedral to conform with the optical and Guinier data. Of the two possible rhombohedral groups (Fig. 3), $R3c$ could be ruled out because the superstructure reflections, recorded by the single-crystal diffractometer, violate the extinction requirements of that group. Thus the correct space group is $R3$.

Structure refinements

In order to obtain an estimate of the structural differences of the three forms of $Li_4B_7O_{12}Cl$, the $F\bar{4}3c$ subcell data of the α and β forms were processed as

described above for the γ form. The results are summarized in Table 2. It can be seen that the average (subcell) structure of the β form is very similar to the prototype (γ) structure. A striking difference is the transfer of Li atoms from the 32(e) to the 24(c) position upon cooling from the γ to the β form. The overall Li content calculated from the occupational parameters is again very close to the formula composition ($0{\cdot}278 \times 32/8 + 0{\cdot}967 \times 24/8 = 4{\cdot}013$ Li atoms per formula unit). The average structure of the room-temperature (α) form, however, is not as well described by the subcell. For this reason the occupancies of the Li positions were held at the ideal values in the least-squares refinement.

An attempt was also made to determine the full structure of β-$Li_4B_7O_{12}Cl$. The intensities of the superstructure reflections are more than two orders of magnitude weaker than the intensities of the subcell reflections. Thus the superstructure can only be due to very subtle variations of the subcell. In the subcell the thermal parameters of the B_7O_{12} framework are normal and quite low. Therefore this framework cannot contribute much to the superstructure. The only possibilities for structural changes are concealed in the occupancy and thermal parameters of the Li atoms and, to a lesser degree, in the thermal parameter of Cl. Several displacive and occupational variations of these atoms were tried in the least-squares refinement of the full data set in space group $P\bar{4}3n$. However, due to the many parameter interactions and probably also because of the poor counting statistics for the superstructure reflections, no entirely satisfactory refinement was achieved. The best results were obtained for a superstructure with ordering of the Li(1) atoms. The ideal occupancy for these atoms in the subcell ($F\bar{4}3c$) is 25% for position 32(e). In the superstructure this position splits into positions 8(e) and 24(i) of $P\bar{4}3n$. For a refinement with position 8(e) fully occupied and position 24(i) empty, an overall R (on F's) of 0·084 was obtained for 552 unique reflections. R for 400 superstructure reflections with counting statistics better than 2σ was 0·31. Even though this refinement probably led to a wrong minimum, the shifts in positional parameters of the O atoms with respect to occupied and empty Li positions were in the right directions considering electrostatic and bond strength–bond length arguments (Brown & Shannon, 1973). Thus the γ–β phase transition at 348 K is probably due to an ordering of the Li(1) atoms.

For the other transition, at 310 K, the freezing-in of the Li(2) atoms at one or the other extremes of their thermal amplitudes is probably responsible. Levasseur, Lloyd, Fouassier & Hagenmuller (1973) have refined the subcell of α-$Li_4B_7O_{12}Cl$ from room-temperature single-crystal data in space group $F23$. They obtained a good fit with split Li(2) atoms (designated by them as Li_1). The superstructure of the α form thus probably corresponds to ordered Li(1) and Li(2) atoms in the primitive, rhombohedrally distorted cell. It remains undetermined.

Ionic conductivity

The Li^+ ions in γ-$Li_4B_7O_{12}Cl$ have large vibrational amplitudes which indicate their loosely bound nature. In addition, the structure provides channels which allow easy diffusion between the various Li sites. Furthermore the Li positions are partially occupied, which suggests a low activation energy for the diffusion process, since the Li^+ ions can move from one site to the other independently. These structural characteristics are typical of fast ionic conductors (Geller, 1972; Armstrong, Bulmer & Dickinson, 1973; Roth & Muller, 1974), and this prompted our investigation of Li^+ conductivity in the Li boracites (Bither & Jeitschko, 1975).

Dielectric measurements

Single crystals of the Li haloboracites were electroded either with a commercial Ag paste or *via* Au sputtering. Conductance and capacitance of the crystals were measured with an automatic capacitance bridge (Hewlett Packard model 4270A) at frequencies ranging from 10^3 to 10^6 Hz. Data were normally taken continuously at increasing temperature after first cooling to liquid-nitrogen temperature. The $Li_4B_7O_{12}X$ crystals all showed unusually high conductance at temperatures above the pseudocubic-to-cubic transition.

Typical results of measurements taken at 10^5 Hz for two crystals are given in Fig. 4. The room-temperature conductivity of $Li_4B_7O_{12}Cl_{0{\cdot}68}Br_{0{\cdot}32}$ is unusually high since it is already in the highly conducting, high-temperature phase (γ form). On the assumption that the conductance thus measured correlates with the AC conductivity, we have plotted the data in the form log σT *vs* $10^3/T$. The slope of the high-temperature portions of the plot in Fig. 4 indicates an activation energy, E_a, of about 0·5 eV, where E_a is defined by $\sigma T = \sigma_0 \exp(-E_a/kT)$. Measurements on a polycrystalline pellet of this same material gave the somewhat higher value for E_a of about 0·6 eV (Shannon, Taylor, English & Berzins, 1977).

The ionic character of the conduction process is indicated by the change of capacitance with frequency. Well below the transition temperature the measured capacitance is frequency independent, but above the transition temperature it varies with frequency, increasing by three orders of magnitude over the range from 10^6 to 10^3 Hz. Figs. 5 and 6 show capacitance *vs* temperature for crystals of $Li_4B_7O_{12}Cl$, $Li_4B_7O_{12}Cl_{0{\cdot}68}Br_{0{\cdot}32}$ and $Li_4B_7O_{12}Br$ at various frequencies.

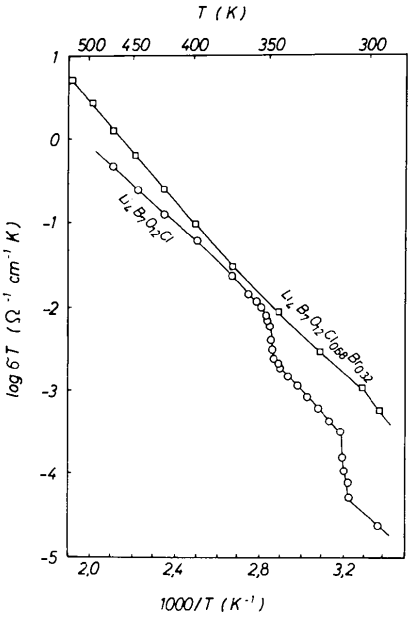

Fig. 4. Conductivity of Li boracites measured with an alternating current of 10^5 Hz.

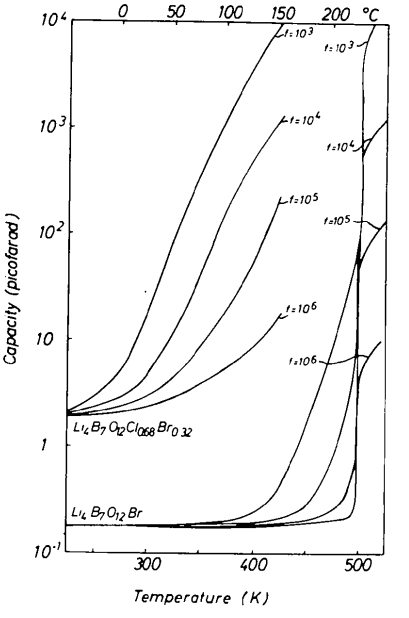

Fig. 6. Capacitance *vs* temperature for crystals of $Li_4B_7O_{12}Cl_{0.68}Br_{0.32}$ and $Li_4B_7O_{12}Br$ at frequencies f (Hz).

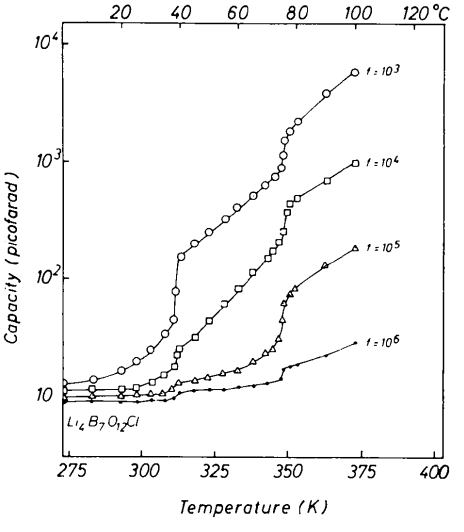

Fig. 5. Capacitance *vs* temperature for a crystal of $Li_4B_7O_{12}Cl$ at various frequencies f (Hz).

DC measurements

The DC ionic conductivity was demonstrated by the use of an electrochemical concentration cell, composed of (1) a saturated Li amalgam in one leg and (2) a 0·1 saturated Li amalgam (1 part saturated amalgam, 9 parts Hg) in the other. The two amalgams were separated by a platelet of $Li_4B_7O_{12}Cl_{0.68}Br_{0.32}$. This cell produced an open-circuit voltage of 68 mV, measured by a high-impedance voltmeter between the two legs, and showed a direct-current conductance of about $10^{-7}\ \Omega^{-1}$.

When the solid-electrolyte crystal was replaced by a liquid ionic conductor comprising $LiClO_4$ dissolved in an organic solvent, the open-circuit voltage was scarcely different (70 mV), indicating ionic conduction in the Li haloboracite. Opposing surfaces of the crystal were then sputtered with Au and the direct-current conductance now measured less than $10^{-10}\ \Omega^{-1}$, indicating that the electronic component of the DC conductivity was no more than a thousandth of the ionic component.

A primary battery comprising a Li haloboracite solid electrolyte was constructed (Fig. 7). The solid electrolyte was $Li_4B_7O_{12}Cl_{0.68}Br_{0.32}$. After assembly of the

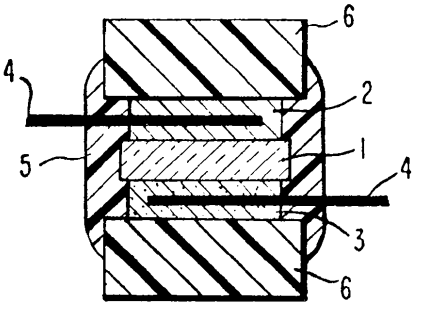

Fig. 7. A primary battery comprising a Li haloboracite solid electrolyte. In this drawing (1) is a Li haloboracite material, (2) is a Li foil anode wrapped around a Pt wire (4), (3) is a cuprous sulfide cathodic layer compacted around a Pt wire, (5) is a commercial potting resin and (6) is a mounting block of poly(methyl methacrylate).

two electrodes and mounting blocks around the crystal, the sandwich was compressed to ensure intimate contact and, while compressed, was hermetically sealed by the potting resin with only the Pt wire terminals exposed. The assembly produced an open-cell voltage of 2·0 V when measured by a high-impedance voltmeter, and showed good shelf stability.

Discussion

Common to all boracites is the B_7O_{12} framework. Interatomic B(1)–O distances are the same (1·470 ± 0·005 Å) for the well refined cubic boracites $Mg_3B_7O_{13}Cl$ (Sueno, Clark, Papike & Konnert, 1973), $Cr_3B_7O_{13}Cl$ (Nelmes & Thornley, 1974), $Ni_3B_7O_{13}I$ (Nelmes & Thornley, 1976) and γ-$Li_4B_7O_{12}Cl$. A difference arises in the Li boracites through the absence of the O atoms at position 8(*a*) of $F\bar{4}3c$. In the cubic boracites with divalent metals these O atoms are rather loosely bonded to four B(2) atoms forming a regular tetrahedron. B(2) thus obtains a trigonally distorted tetrahedral O coordination formed by three O atoms of the general position at 1·435 ± 0·002 Å and one of position 8(*a*) at 1·683 ± 0·010 Å (these values are the average distances in the three well refined cubic boracites $M^{II}_3B_7O_{13}X$ cited above). In γ-$Li_4B_7O_{12}Cl$, through the absence of its fourth O atom, B(2) moves towards the center of the triangle formed by its remaining O atoms, thus shortening its distances to these three from 1·43 to 1·37 Å which is the usual distance in BO_3 groups. The missing O atom of $Li_4B_7O_{12}Cl$ has large displacements in the phase transitions (and, therefore, also in the ferroelectric–ferroelastic switching processes) of $M^{II}_3B_7O_{13}X$ boracites, thereby changing the O coordination of the B(2) atoms between trigonal and distorted tetrahedral (Dowty & Clark, 1973; Thornley, Nelmes & Kennedy, 1976). Since this O atom is missing in the Li boracites, it cannot be responsible for their phase transitions.

Li(2) of γ-$Li_4B_7O_{12}Cl$ corresponds to Mg in $Mg_3B_7O_{13}Cl$. Its site symmetry is $\bar{4}$ with four O neighbors forming approximately a square and two Cl atoms along the fourfold axis completing a stretched octahedron. The Li(2)–O distances have the expected value. The Li(2)–Cl distances, however, are about 0·5 Å greater than the sum of the ionic radii. This unusual coordination is reflected in the large thermal amplitudes of Li(2). Its r.m.s. displacements along the fourfold axis are 0·45 Å. It is likely that the Li(2) atoms move in a double minimum potential. An indication of this was obtained in the final difference synthesis which showed a negative electron density corresponding to −0·14 Li atoms at the site of Li(2). Similar anisotropic motion was observed for Mg in $Mg_3B_7O_{13}Cl$ (Sueno *et al.*, 1973), for Cr in $Cr_3B_7O_{13}Cl$ (Nelmes & Thornley, 1974), and for Ni in $Ni_3B_7O_{13}I$ (von Wartburg, 1974; Nelmes & Thornley, 1976). There, however, the r.m.s. displacements are only about half as large as for γ-$Li_4B_7O_{12}Cl$, and a double minimum potential for the metal atoms in these compounds is disputed (Thornley, Kennedy & Nelmes, 1976).

The halogen ion is situated in the center of a large cavity of the B_7O_{12} framework. This cavity is large enough to accommodate the additional Li(1) ion. It is statistically distributed over four sites forming a tetrahedron around the halogen. Its near-neighbor environment has point symmetry 3 and consists of three O and one Cl forming a distorted tetrahedron. At any given moment Li(1) will, of course, occupy only one of the four equivalent sites, thereby displacing the Cl atom from its ideal position. The relatively large temperature factor of Cl is thus explained.

It is interesting that the average structure of β-$Li_4B_7O_{12}Cl$, as indicated by the subcell refinement, is so similar to the structure of the γ phase. The main differences are in the occupancy parameters of the Li positions. The ideal occupancy values for a fully ordered structure would be $\frac{1}{4}$ for position 32(*e*) and 1 for position 24(*c*). Apparently (extrapolating from our data), these occupancies are obtained only at low temperatures for the subcell when the compound is in the α form. As the temperature is raised, more and more Li ions move from position 24(*c*) to position 32(*e*). This is also indicated by the high ionic conductivity at high temperatures.

The room-temperature conductivity of the best conducting composition $Li_4B_7O_{12}Cl_{0.68}Br_{0.32}$ is 2×10^{-6} Ω^{-1} cm^{-1}. At 520 K the conductivity for this composition is raised to $0{\cdot}9 \times 10^{-2}$ Ω^{-1} cm^{-1}. This compares to a value of $0{\cdot}3 \times 10^{-2}$ Ω^{-1} cm^{-1} at this temperature for Li β-alumina (Whittingham & Huggins, 1972), the best Li^+ conductor known (McGeehin & Hooper, 1977). Recent AC measurements on ionic conductivity of the Li boracites with a different experimental technique resulted in even higher values (Réau, Levasseur, Magniez, Calès, Fouassier & Hagenmuller, 1976). Our conductivity values are possibly somewhat low due to polarization effects at the ionically non-conducting electrodes.

Because of their greater experimental simplicity, temperature-dependent measurements on ionic conductivity are frequently carried out with AC techniques. These techniques do not distinguish between ionic transport over large distances and the rattling of ions in cages formed by the framework of the structure. For long-range ionic transport in the Li boracites the Li^+ ions need to move alternatingly between Li(1) and Li(2) sites. Thus the long-range (DC) conductivity is limited by the mobility of the slower moving species. Our DC measurements prove the ionic character of the conduction process. A DC study at various temperatures would be needed to distinguish the various contributions to the AC conductivity.

We acknowledge D. M. Graham's enthusiastic help with the crystallographic work.

References

ARMSTRONG, R. D., BULMER, R. S. & DICKINSON, T. (1973). *J. Solid State Chem.* **8**, 219–228.

BITHER, T. A. & JEITSCHKO, W. (1975). US Patent 3 911 085 (applied 23 October 1973, allowed 7 October 1975); *Chem. Abs.* (1976), **84**, 33572*a*.

BOYD, F. R. & ENGLAND, J. L. (1960). *J. Geophys. Res.* **65**, 741–748.

BROWN, I. D. & SHANNON, R. D. (1973). *Acta Cryst.* A**29**, 266–282.

COPPENS, P. & VOS, A. (1971). *Acta Cryst.* B**27**, 146–158.

CROMER, D. T. & LIBERMAN, D. (1970). *J. Chem. Phys.* **53**, 1891–1898.

CROMER, D. T. & MANN, J. B. (1968). *Acta Cryst.* A**24**, 321–324.

DOWTY, E. & CLARK, J. R. (1973). *Z. Kristallogr.* **138**, 64–99.

FINGER, L. W. (1969). An unpublished computer program for the least-squares refinement of crystal structures.

FRITCHIE, C. J. & GUGGENBERGER, L. J. (1967). An unpublished electron density summation program.

GELLER, S. (1972). *Fast Ion Transport in Solids*, Conf. Proc., edited by W. VAN GOOL, pp. 609–616 (published 1973). Amsterdam: North-Holland.

GÖTTLICHER, S. & WÖLFEL, W. (1959). *Z. Electrochem.* **63**, 891–901.

ITO, T., MORIMOTO, N. & SADANAGA, R. (1951). *Acta Cryst.* **4**, 310–316.

JEITSCHKO, W. (1972). *Acta Cryst.* B**28**, 60–76.

JEITSCHKO, W. & BITHER, T. A. (1972). *Z. Naturforsch.* **27b**, 1423.

JOHNSON, C. K. (1965). *ORTEP.* Report ORNL-3794. Oak Ridge National Laboratory, Tennessee.

LEVASSEUR, A., FOUASSIER, C. & HAGENMULLER, P. (1971). *Mater. Res. Bull.* **6**, 15–22.

LEVASSEUR, A., LLOYD, D. J., FOUASSIER, C. & HAGENMULLER, P. (1973). *J. Solid State Chem.* **8**, 318–324.

MCGEEHIN, P. & HOOPER, A. (1977). *J. Mater. Sci.* To be published.

NELMES, R. J. (1974). *J. Phys. C: Solid State Phys.* **7**, 3840–3854.

NELMES, R. J. & THORNLEY, F. R. (1974). *J. Phys. C: Solid State Phys.* **7**, 3855–3874.

NELMES, R. J. & THORNLEY, F. R. (1976). *J. Phys. C: Solid State Phys.* **9**, 665–680.

O'CONNELL, A. M., RAE, A. I. M. & MASLEN, E. N. (1966). *Acta Cryst.* **21**, 208–219.

RÉAU, J.-M., LEVASSEUR, A., MAGNIEZ, G., CALÈS, B., FOUASSIER, C. & HAGENMULLER, P. (1976). *Mater. Res. Bull.* **11**, 1087–1090.

ROTH, W. L. & MULLER, O. (1974). *The Study, Selection and Preparation of Solid-State Cationic Conductors.* NASA Report CR-134610.

SHANNON, R. D., TAYLOR, B. E., ENGLISH, A. D. & BERZINS, T. (1977). *Mater. Res. Bull.* To be published.

SUENO, S., CLARK, J. R., PAPIKE, J. J. & KONNERT, J. A. (1973). *Amer. Min.* **58**, 691–697.

THORNLEY, F. R., KENNEDY, N. S. J. & NELMES, R. J. (1976). *J. Phys. C: Solid State Phys.* **9**, 681–692.

THORNLEY, F. R., NELMES, R. J. & KENNEDY, N. S. J. (1976). Private communication.

WARTBURG, W. VON (1974). *Phys. Stat. Sol.* (*a*). **21**, 557–568.

WHITTINGHAM, M. S. & HUGGINS, R. A. (1972). *Solid-State Chemistry*, Proc., pp. 139–154. NBS Spec. Publ. 364.

ZACHARIASEN, W. H. (1963). *Acta Cryst.* **16**, 1139–1144.